Scientific Research Publishing

World Journal of Engineering and Technology, 2023, 11, 20-40
https://www.scirp.org/journal/wjet
ISSN Online: 2331-4249
ISSN Print: 2331-4222

Contribution to Asymmetrical Compensation through Parallel Controllers of FACTS (STATCOM)—IPC 240 Dual for a Power Transmission Line

Kengne Chatue Charlène Steva, Mengata Mengounou Ghislain, Koko Koko Joseph, Batassou Guilzia Jeannot, Nneme Nneme Leandre

Laboratory of Computer and Automatic Engineering, UFD of Engineering Sciences, ENSET, University of Douala, Douala, Cameroon
Email: charlene.chatue@yahoo.fr, mengata@univ-douala.com, kokojoseph469@yahoo.fr, batassoujeannot@yahoo.fr, leandren@gmail.com

How to cite this paper: Steva, K.C.C., Ghislain, M.M., Joseph, K.K., Jeannot, B.G. and Leandre, N.N. (2023) Contribution to Asymmetrical Compensation through Parallel Controllers of FACTS (STATCOM)—IPC 240 Dual for a Power Transmission Line. *World Journal of Engineering and Technology*, **11**, 20-40.
https://doi.org/10.4236/wjet.2023.111003

Received: July 22, 2022
Accepted: January 15, 2023
Published: January 18, 2023

Abstract

This work is part of the resolution of problems encountered on a 225 KV MANGOMBE-OYOMABANG line. This line is characterized by important technical losses, so that the voltage injected in the busbar is always lower than 200 kV. The main objective of this work is to show the new solutions that can provide a combined FACTS-STATCOM and IPC 240 dual system on this line. Then to show the limitation of STATCOM compared to RPI 240. The results obtained allowed us to observe that in symmetrical operation the STATCOM improves the voltage profile on the busbar and in asymmetrical operation we found that it continues to regulate the voltage of each phase despite the unbalance. But the system remains too unbalanced because of the sequence current flow. The IPC 240 corrects this limitation, allowing asymmetrical operation of the line in an emergency while providing continuous service to the load.

Keywords

FACTS, STATCOM, IPC 240 Dual, Symmetry, Asymmetry, Contingency, Voltage Profile

1. Introduction

For several years, electrical energy producers have been striving to guarantee the quality of electrical energy, the first efforts have focused on continuity of service and then on compensation technology by FACTS (Flexible Alternative Current

Transmission System) in order to always make access to energy available to the user. They are electronic or static systems that allow the adjustment of one or more parameters of the network, they are used to control the distribution of loads in the network, thus improving the transit capacity and reducing losses, to control the voltage in one point or ensure the dynamic stability of the electricity transmission networks and the production groups connected to them. Current Flexible Alternating Current Transmission Systems (FACTS) cannot handle the widespread problem of high short circuit levels on power transmission lines [1]. The traditional solution, which consists of splitting the networks, undermines their operating flexibility and even their reliability. The Interphase Power Regulator (IPR) is an innovative solution for environments with high short-circuit levels; they are part of the current of thought of the concept of FACTS networks. It will be a question for us of modeling and simulating via the simulation software MATLAB Simulink the STATCOM and the IPC 240 dual with three branches, in order to show the limit of the STATCOM compared to the IPC 240.

2. Materials and Methods

2.1. Materials

FACTS are auxiliary power electronic equipment used to control load distribution in the network, thus improving the transit capacity and reducing losses, to control the voltage at a point or ensure the dynamic stability of electricity transmission networks and production groups connected to them. The development of IPC technology was mainly motivated by the need to create new power flow controllers to overcome network operating limitations caused by too high short-circuit levels [2].

As materials we used; the Matlab Simulink software as simulation software which allowed us to test our model and a PC as a working tool (**Table 1**).

2.2. Methods

2.2.1. Statcom Modeling

For the simplified modeling of the STATCOM it is assumed that the DC circuit consists of a constant voltage source. In this model the equivalent circuit will be represented as follows (**Figure 1**).

Considering that:

$$\bar{V}_{sh}^{(d,q)} = V_{shd} + jV_{shq} = v\cos\theta + jv\sin\theta \quad (1)$$

V: being the modulus of the injected voltage which depends directly on the DC voltage U_{dc} and can be expressed by [4]:

$$V = m * U_{dc} \quad (2)$$

Table 1. Characteristics of the MANGOMBE-OYOMABANG transmission line [3].

Line	Type	Level [kV]	Length [km]	R1 (ohm)	X1 [Ω]	B1 [μS]	R0 [Ω]	X0 [Ω]	B0 [μS]	IMAX [A]
Man-Oyo	ALMELEC 225,366 mm^2	225	168	14.77	69.72	460.15	15.72	140.62	249.48	600

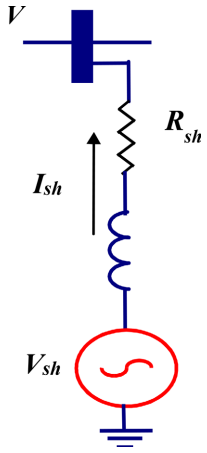

Figure 1. Equivalent diagram of STATCOM [4].

m: is the modulation index it only depends on the type of inverter. Substituting Equations (2) and (1) we get:

$$\begin{aligned} V_d - mU_{dc}\cos\theta &= R_{sh}\cdot I_{shd} + L_{sh}\cdot\frac{\mathrm{d}I_{shd}}{\mathrm{d}t} - L_{sh}\cdot I_{shq} \\ V_d - mV_{dc}\sin\theta &= R_{sh}\cdot I_{shq} + L_{sh}\cdot\frac{\mathrm{d}I_{shq}}{\mathrm{d}t} - L_{sh}\cdot I_{shd} \end{aligned} \tag{3}$$

The power flowing between the capacitor and the voltage inverter can be described by Equation (4) and at the same time verify the following equality:

$$\begin{aligned} P_{sh} &= \frac{3}{2}\left(V_{shd}\cdot I_{shd} + V_{shq}\cdot I_{shq}\right) \\ U_{dc}I_{dc} &= \frac{3}{2}\left(V_{shd}\cdot I_{shd} + V_{shq}\cdot I_{shq}\right) \end{aligned} \tag{4}$$

The current I_{dc} is defined as being the sum of the capacitive current "ic" and the resistive current "irc" in the branch of the resistor R_{dc}.

$$I_{dc} = C\frac{\mathrm{d}U_{dc}}{\mathrm{d}t} + \frac{U_{dc}}{R_c} \tag{5}$$

From these equations we can derive the dynamic equation of the continuous side of the following STATCOM:

$$C\frac{\mathrm{d}U_{dc}}{\mathrm{d}t} = \frac{3}{2}m\left(I_{shd}\cos\theta + I_{shq}\sin\theta\right) - \frac{U_{dc}}{R_c} \tag{6}$$

Previous equations form the state equation system of STATCOM taking into account the variations of the voltage of the DC circuit which is written in the following matrix form.

$$\frac{\mathrm{d}}{\mathrm{d}t}\begin{bmatrix} I_{shd} \\ I_{shq} \\ U_{dc} \end{bmatrix} = \begin{bmatrix} \frac{-R}{L_{sh}} & 0 & \frac{-m}{L_{sh}}\cos\theta \\ -\omega & \frac{-R}{L_{sh}} & \frac{-m}{L_{sh}}\sin\theta \\ \frac{3}{2}\frac{m}{c}\cos\theta & -\frac{3}{2}\frac{m}{c}\sin\theta & \frac{1}{R_{eC}} \end{bmatrix}\begin{bmatrix} I_{shd} \\ I_{shq} \\ U_{dc} \end{bmatrix} + \begin{bmatrix} \frac{1}{L_{sh}} & 0 \\ 0 & \frac{1}{L_{sh}} \\ 0 & 0 \end{bmatrix}\begin{bmatrix} V_d \\ V_q \end{bmatrix} \tag{7}$$

It can be observed that there are two control parameters in this system with three state parameters to be controlled and only two quantities can be controlled independently. This system that must be linearized around an operating point will be of the following form:

$$\frac{\mathrm{d}}{\mathrm{d}t}\begin{bmatrix} I_{shd} \\ I_{shq} \\ U_{dc} \end{bmatrix} = \begin{bmatrix} \frac{-R}{L_{sh}} & 0 & \frac{-m}{L_{sh}}\cos\theta_0 \\ -\omega & \frac{-R}{L_{sh}} & \frac{-m}{L_{sh}}\sin\theta_0 \\ \frac{3}{2}\frac{m}{c}\cos\theta_0 & -\frac{3}{2}\frac{m}{c}\sin\theta_0 & \frac{1}{R_{eC}} \end{bmatrix}\begin{bmatrix} I_{shd} \\ I_{shq} \\ U_{dc} \end{bmatrix} + \begin{bmatrix} \frac{1}{L_{sh}} & 0 & \frac{m}{L_{sh}}U_{dc0}\sin\theta_0 \\ 0 & \frac{1}{L_{sh}} & \frac{m}{L_{sh}}U_{dc0}\cos\theta_0 \\ 0 & 0 & -\frac{3}{2}\frac{m}{c}\left(I_{shd}\sin\theta_0 + I_{shq}\cos\theta_0\right) \end{bmatrix}\begin{bmatrix} V_d \\ V_q \\ \theta \end{bmatrix} \tag{8}$$

The reactive current is controlled independently to control the reactive power flow and the other parameters are used to keep the DC voltage U_{dc} constant.

2.2.2. Determination of References

Considering the simplified model represented by the system of Equation (8) above [5]:

$$\frac{\mathrm{d}}{\mathrm{d}t}\begin{bmatrix} I_{shd} \\ I_{shq} \end{bmatrix} = \begin{bmatrix} -\frac{R_{sh}}{L_{sh}} & w \\ -w & -\frac{R_{sh}}{L_{sh}} \end{bmatrix}\cdot\begin{bmatrix} I_{shd} \\ I_{shq} \end{bmatrix} + \frac{1}{L_{sh}}\cdot\begin{bmatrix} V_d & -V_{shd} \\ V_q & -V_{shq} \end{bmatrix} \tag{9}$$

On the control vector, the following change of variable is made:

$$\frac{1}{L_{sh}}\cdot\begin{bmatrix} V_d & -V_{shd} \\ V_q & -V_{shq} \end{bmatrix} = \begin{bmatrix} X_1 \\ X_2 \end{bmatrix}5 \tag{10}$$

With;

$$X_2 = \frac{1}{L_{sh}}\left(V_d - V_{shq}\right) \tag{11}$$

and;

$$X_1 = \frac{1}{L_{sh}}\left(V_q - V_{shq}\right) \tag{12}$$

Are the new command quantities. From the first equation of the system (10) we will have:

$$\frac{\mathrm{d}I_{shd}}{\mathrm{d}t} = -\frac{R_{sh}}{L_{sh}}I_{shd} + w\cdot I_{shq} + X_1 \tag{13}$$

By applying the Laplace transformation to this equation, we obtain:

$$\left(S+\frac{R_{sh}}{L_{sh}}\right)I_{shd}=w\cdot I_{shq}+X_1 \tag{14}$$

From where we arrive at the transfer according to the following:

$$\frac{I_{shq}}{\tilde{X}_1}=\frac{1}{S+\dfrac{R_{sh}}{L_{sh}}} \tag{15}$$

Our order in reality is in X_1 and like $\tilde{X}_1=\omega\cdot I_{shq}+X_1$, we must therefore add the term $\omega\cdot I_{shq}$ to find $\tilde{X}_1$ at the input of this transfer as shown in the diagram in the following **Figure 2**.

In the same way, taking the second equation of the previous model, we find the transfer I_{shq} in terms of $\tilde{X}_2$ following:

$$\frac{I_{shq}}{\tilde{X}_2}=\frac{1}{S+\dfrac{R_{sh}}{L_{sh}}} \tag{16}$$

With,

$$\tilde{X}_2=\omega I_{shd}+X_2 \tag{17}$$

The following diagram summarizes this transfer (**Figure 3**).

From what we have just seen we see that there is a natural coupling in the transfers of Currents I_{shd} and I_{shq}.

To eliminate this coupling, we use the compensation method and with PI regulators, we can control the output currents of the STATCOM and make them follow their instructions I_{shd} and I_{shq} as shown in the block diagram of **Figure 4**.

In the same way for the reactive current we must add the component $\omega\cdot I_{shd}$ and finally arrived at the STATCOM regulation scheme by the decoupled Watt-Var method of **Figure 5**.

2.2.3. Modeling of the Rpi 240 for Asymmetric Compensation of Transmission Lines

The topology of a transmission line equipped with dual RPIs is shown in **Figure 6**.

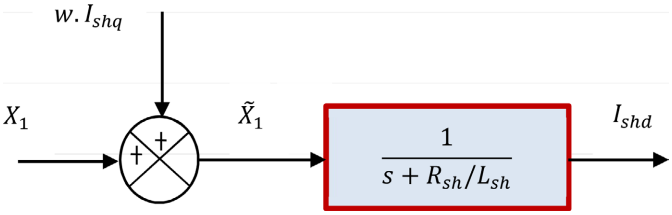

Figure 2. I_{shd} transfer as a function of X_1 [6].

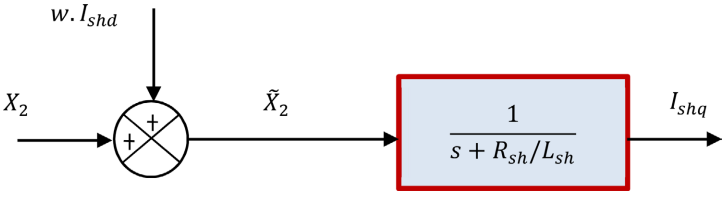

Figure 3. I_{shq} transfer as a function of X_2 [6].

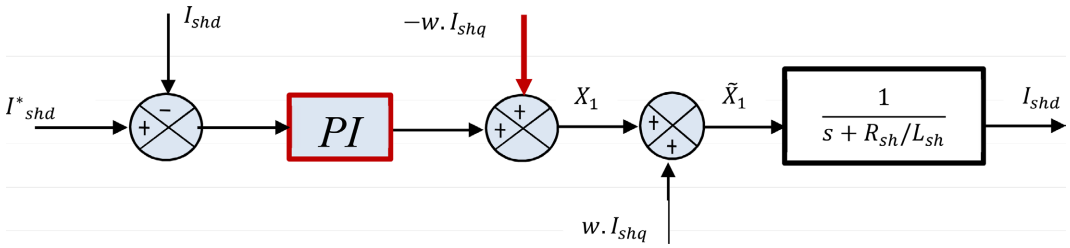

Figure 4. Regulation and decoupling of I_{shd} [6].

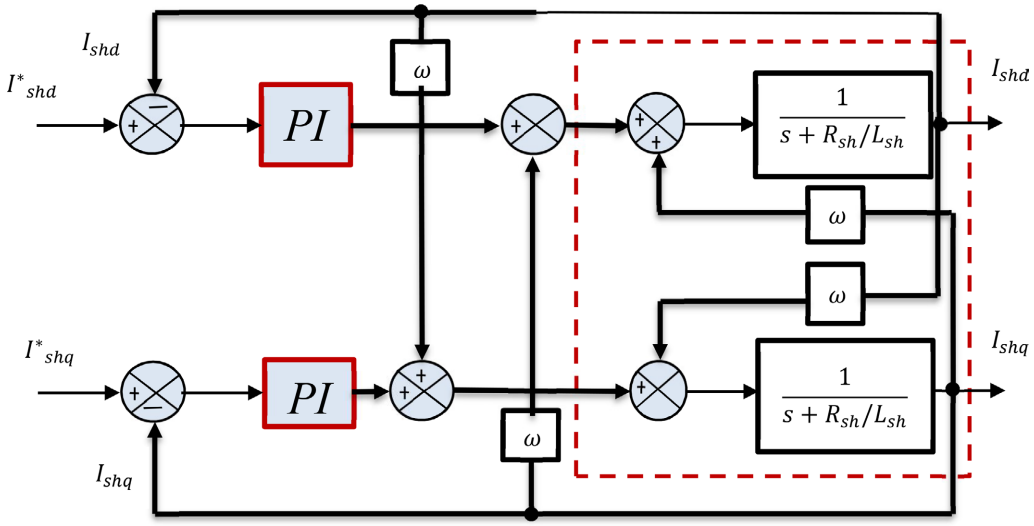

Figure 5. STATCOM Regulation Schematic (Watt-Var decoupled) [6].

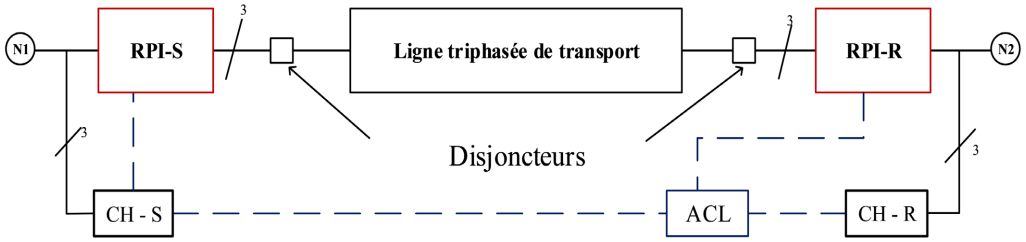

Figure 6. Topology of a power transmission line equipped with dual IPCs [7].

- N1 and N2: connection nodes to the energy source and to the load.
- RPI-S, RPI-R: RPI connected to source and load respectively.
- ACL: Logic control automaton for the synchronization of the two RPIs.
- D1 to D6: Intelligent circuit breaker with single-phase tripping.
- Is_X: RPI-S input current intensity for phases X ϵ [1].
- Ir_X: Current intensity towards the load for phases X ϵ [1].

2.2.4. Dimensions of the Elements of the RPI 240 Has Three Branches

We will use the Fortescue transformation in order to simplify the analysis of the unbalanced three-phase electrical system. This is mathematically a basic change. The basic idea is that an asymmetric system of N phrasers (3 for three-phase) can be decomposed as the sum of N symmetric systems. The Fortescue transformation is thus also called the method of symmetric components. A three-phase system,

whether currents, voltages, fluxes, etc., is thus broken down into three balanced (or symmetrical) systems: Direct, Inverse, Homopolar [8]. Let's pose

$$F = \begin{bmatrix} 1 & 1 & 1 \\ a^2 & a & 1 \\ a & a^2 & 1 \end{bmatrix} \tag{18}$$

Fortescue's Matrix

$$\mathrm{Vs}_{\_abc} = \begin{pmatrix} \mathrm{Vs}_{\_A} \\ \mathrm{Vs}_{\_B} \\ \mathrm{Vs}_{\_C} \end{pmatrix}; \quad \mathrm{Vr}_{\_abc} = \begin{pmatrix} \mathrm{Vr}_{\_A} \\ \mathrm{Vr}_{\_B} \\ \mathrm{Vr}_{\_C} \end{pmatrix} \tag{19}$$

The simple voltage vectors at the source (s) and at the load (r) of a power transmission line.

$$\mathrm{Vs}_{\_120} = \begin{pmatrix} \mathrm{Vs}_{\_A1} \\ \mathrm{Vs}_{\_A2} \\ \mathrm{Vs}_{\_A0} \end{pmatrix}; \quad \mathrm{Vr}_{\_120} = \begin{pmatrix} \mathrm{Vr}_{\_A1} \\ \mathrm{Vr}_{\_A2} \\ \mathrm{Vr}_{\_A0} \end{pmatrix} \tag{20}$$

The source and load voltage vectors of the forward (1) and reverse (2) systems of a transmission line. The same for the current intensities

$$\mathrm{Is}_{\_abc} = \begin{pmatrix} \mathrm{Is}_{\_A} \\ \mathrm{Is}_{\_B} \\ \mathrm{Is}_{\_C} \end{pmatrix}; \quad \mathrm{Ir}_{\_abc} = \begin{pmatrix} \mathrm{Ir}_{\_A} \\ \mathrm{Ir}_{\_B} \\ \mathrm{Ir}_{\_C} \end{pmatrix} \tag{21}$$

The source and load line current intensities vectors on a transmission line.

$$\mathrm{Is}_{\_120} = \begin{pmatrix} \mathrm{Is}_{\_A1} \\ \mathrm{Is}_{\_A2} \\ \mathrm{Is}_{\_A0} \end{pmatrix}; \quad \mathrm{Ir}_{\_120} = \begin{pmatrix} \mathrm{Ir}_{\_A1} \\ \mathrm{Ir}_{\_A2} \\ \mathrm{Ir}_{\_A0} \end{pmatrix} \tag{22}$$

The symmetrical components of source and load currents of a transmission line [9].

For the tensions

$$\begin{aligned} \mathrm{Vs}_{\_120} &= F^{-1}\mathrm{Vs}_{\_abc} \\ \mathrm{Vr}_{\_120} &= F^{-1}\mathrm{Vr}_{\_abc} \end{aligned} \tag{23}$$

For the intensities

$$\begin{aligned} \mathrm{Is}_{\_120} &= F^{-1}\mathrm{Is}_{\_abc} \\ \mathrm{Ir}_{\_120} &= F^{-1}\mathrm{Ir}_{\_abc} \end{aligned} \tag{24}$$

$a = \mathrm{e}^{j2\pi/3}$: Positive rotation vector operator 1, 2, 0: direct, reverse and homopolar system respectively

2.2.5. Sizing of the Reactances of the Inverse System Compensator

This dimensioning can be done in three steps:

Step 1: Calculation of the phase-to-neutral voltage across the terminals of the compensator elements: [10]

$$\begin{aligned}\underline{U}_{AB} &= \underline{V}_A - \underline{V}_B \\ \underline{U}_{BC} &= \underline{V}_B - \underline{V}_C = a^2\underline{U}_{AB} \\ \underline{U}_{CA} &= \underline{V}_C - \underline{V}_A = a\underline{U}_{AB}\end{aligned} \tag{25}$$

By combining this system of equations with that which describes the simple tensions in their symmetrical components, one obtains:

$$\begin{aligned}\underline{V}_{A1} &= \frac{\underline{V}_{AB}\angle -30^\circ}{\sqrt{3}} = \underline{V}_{AN} \\ \underline{V}_{A2} &= 0\end{aligned} \tag{26}$$

The voltage of the direct system V_{A1} at the terminals of the elements of the compensator is equal to the phase-to-neutral voltage at the source V_{AN}, however, V_{An0} remains undetermined [11].

Step 2: Computing the intensity of the compensator current.

$$\begin{aligned}\underline{I}_A &= \underline{I}_{A1} + \underline{I}_{A2} = -\underline{I}_2 \\ \underline{I}_B &= a^2\underline{I}_{A1} + a\underline{I}_{A2} = -a\underline{I}_2 \\ \underline{I}_c &= a\underline{I}_{A1} + a^2\underline{I}_{A2} = -a^2\underline{I}_2\end{aligned} \tag{27}$$

$$I_{A1} = 0;\ I_{A2} = -I_2$$

Step 3: Computing the reactances of the compensator We can rewrite equation:

$$\begin{aligned}\underline{V}_{A1} &= \underline{I}_{A1}\underline{Z}a_0 + \underline{I}_{A2}\underline{Z}a_2 \\ \underline{V}_{A2} &= \underline{I}_{A1}\underline{Z}a_1 + \underline{I}_{A2}\underline{Z}a_0 \\ \underline{V}_{A0} &= \underline{I}_{A1}\underline{Z}a_2 + \underline{I}_{A2}\underline{Z}a_1\end{aligned} \tag{28}$$

$$\begin{aligned}\underline{V}_{A1} &= -\underline{I}_2\underline{Z}a_2 = \underline{V}_{AN} \\ \underline{V}_{A2} &= -\underline{I}_2\underline{Z}a_0 = 0 \\ \underline{V}_{A0} &= -\underline{I}_2\underline{Z}a_1 = ?\end{aligned} \tag{29}$$

From were

$$\underline{Z}a_2 = \frac{\underline{V}_{AN}}{-\underline{I}_2} = R_2 + jX_2 \tag{30}$$

R_2 and X_2 are respectively resistance and reactance of the inverse system.

$$R_2 + jX_2 = 3\frac{V_{AS}}{-\underline{I}_{AS}} = \frac{\frac{225000}{\sqrt{3}}\angle 12^\circ}{3.624\times 10^2 + j1.1751\times 10^2} = 703.8497 - j139.1417 \tag{31}$$

The conclusions of the equations make it possible to write [11]:

$$\begin{aligned}\underline{Z}a &= 0 + jX_a = \underline{Z}a_1 + \left(R_2 + jX_2\right) \\ \underline{Z}b &= 0 + jX_b = a^2\underline{Z}a_1 + a\left(R_2 + jX_2\right) \\ \underline{Z}c &= 0 + jX_c = a\underline{Z}a_1 + a^2\left(R_2 + jX_2\right)\end{aligned} \tag{32}$$

As $a = -0.5 + j\frac{\sqrt{3}}{2}$; $a^2 = -0.5 - j\frac{\sqrt{3}}{2}$ and taking into account the previous equations we obtain:

$$\underline{Z}a_1 = -R_2 + jX_2 \tag{33}$$

From were

$$\begin{aligned} &\underline{Z}a = 0 + jX_a = -R_2 + jX_2 + \left(R_2 + jX_2\right) \\ &\Rightarrow X_a = 2X_2 = -278.2834\,\Omega \end{aligned} \tag{34}$$

$$\underline{Z}b = 0 + jX_b = \left(-0.5 - j\frac{\sqrt{3}}{2}\right)\left(-R_2 + jX_2\right) + \left(-0.5 + j\frac{\sqrt{3}}{2}\right)\left(R_2 + jX_2\right) \tag{35}$$

$$\Rightarrow X_b = \sqrt{3}R_2 - X_2 = 1358.245141\,\Omega$$

$$\underline{Z}c = 0 + jX_c = \left(-0.5 + j\frac{\sqrt{3}}{2}\right)\left(-R_2 + jX_2\right) + \left(-0.5 - j\frac{\sqrt{3}}{2}\right)\left(R_2 + jX_2\right) \tag{36}$$

$$\Rightarrow X_c = -\sqrt{3}R_2 - X_2 = -1079.91174\,\Omega$$

The same developments can be carried out if the fault occurs on phases B and C. Finally, the expressions for the compensation reactances of the reverse system are given in Table 2 according to the contingency phase.

3. Results and Discussion

In this part, we will simulate the STATCOM and RPI 240 dual three-legged devices that were modeled in the previous chapter. These simulations will allow us to show the contribution of the STATCOM and RPI 240 dual three-branch devices in solving the problems encountered by the transmission network managers on the 225 kV MANGOMBE-OYOMABANG line. Thereafter we will present the results of the simulations obtained on MATLAB/Simulink, and finally we will make an interpretation of these results.

3.1. Network Simulation without Compensator

Figure 7 below shows the 225 kV MANGOMBE-OYOMABANG line with a load at MANGOMBE, and another at OYOMABANG. We are interested in the voltage and powers at MANGOMBE and OYOMABANG busbars.

Table 2. Expression of compensator reactances.

Reference phase (faulty)	Expression	Value of retances
A	$X_a = X_{aa} = 2X_2$ $X_b = X_{ba} = \sqrt{3}R_2 - X_2$ $X_c = X_{ca} = -\sqrt{3}R_2 - X_2$	$X_{aa} = 278.2834\,\Omega$ $X_{ba} = 1358.245141\,\Omega$ $X_{ca} = 1079.91174\,\Omega$
B	$X_a = X_{ab} = -\sqrt{3}R_2 - X_2$ $X_b = X_{bb} = 2X_2$ $X_c = X_{cb} = \sqrt{3}R_2 - X_2$	$X_{ab} = 1079.91174\,\Omega$ $X_{bb} = 278.2834\,\Omega$ $X_{cb} = 1358.245141\,\Omega$
C	$X_a = X_{ac} = \sqrt{3}R_2 - X_2$ $X_b = X_{bc} = -\sqrt{3}R_2 - X_2$ $X_c = X_{cc} = 2X_2$	$X_{ac} = 1358.245141\,\Omega$ $X_{bc} = 1079.91174\,\Omega$ $X_{cc} = 278.2834\,\Omega$

3.2. Types of Voltage in Mangombe and Oyomabang (Figure 8)

The first graph displays the three-phase signal of the voltage at MANGOMBE, and the second the voltage at OYOMABANG.

In the presence of the load, the voltage amplitude at OYOMABANG is 1.571×10^5 or 157.1 kV or at MANGOMBE is 1.833×10^5 or 182.9 kV. Thus, a voltage drop is observed which is justified by the inrush of the current of the load which traverses the line (Table 3).

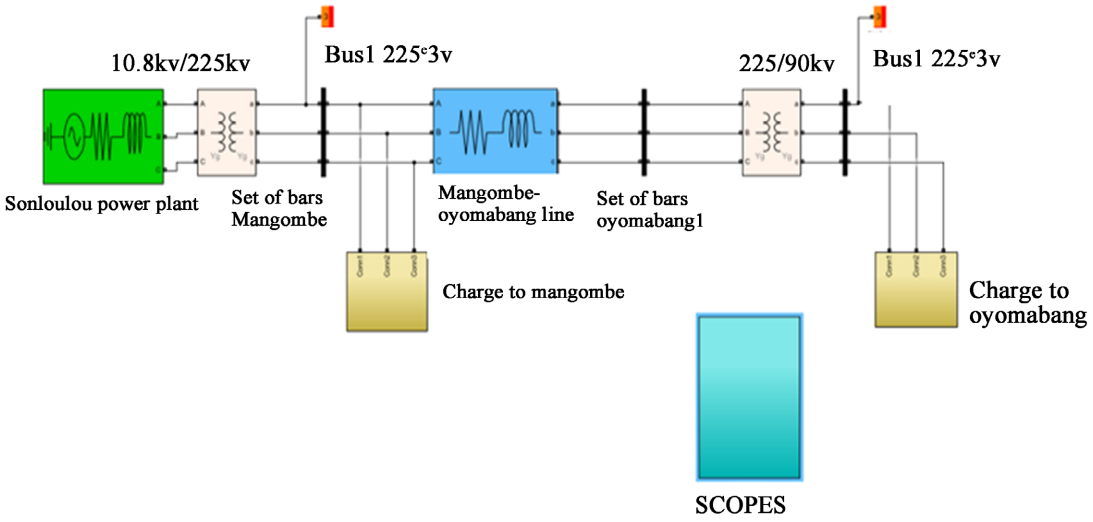

Figure 7. Line model on Simulink.

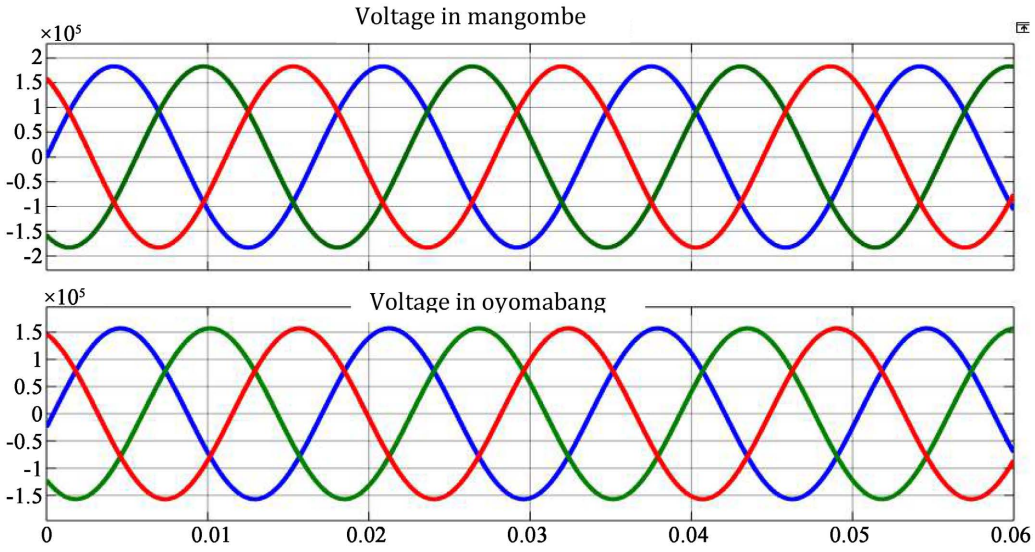

Figure 8. Voltage curves at MANGOMBE and OYOMABANG.

Table 3. Indication of wattmeters.

BUS	Voltage	Active power P	Reactive power Q
MANGOMBE	182.9 kV	1.91×10^8	1.439×10^8
OYOMABANG	157.1 kV	8.772×10^7	5.118×10^7

3.3. Model of the Line with the Statcom (Figure 9)

When the STATCOM is not in operation, the "natural" power flow on the transmission line is 223 MW from bus B1 to B2. This STATCOM is a phasor model of a typical three level PWM STATCOM. The simulation of this model gave the following results.

3.4. Voltage and Current Curves after Insertion of the Statcom in Mangombe and Oyomabang

Figure 10 displays the voltage signal at OYOMABANG before and after insertion of the STATCOM. At the OYOMABANG busbar level, we see a

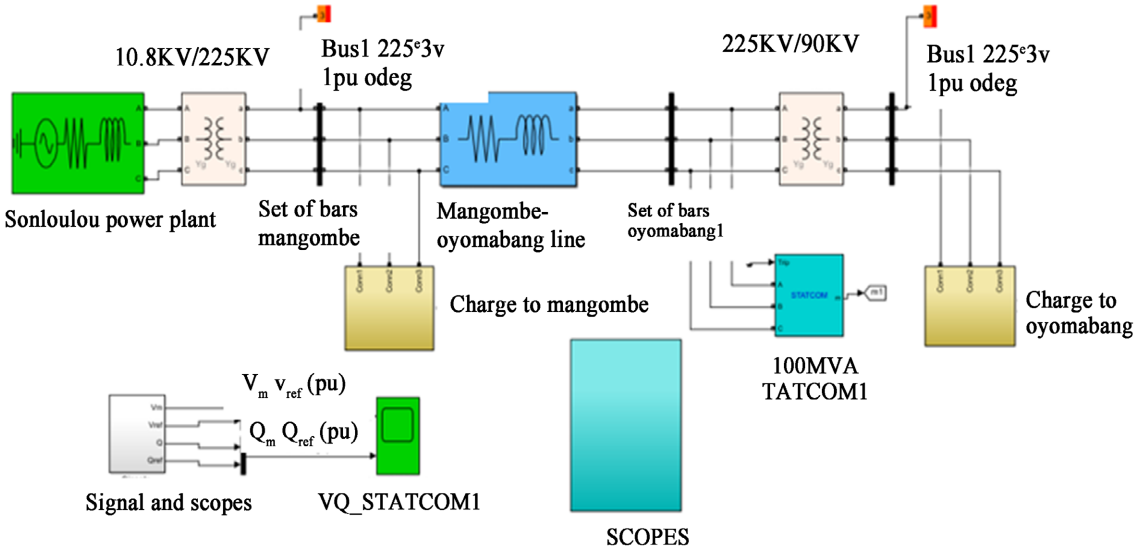

Figure 9. Line model with STATCOM.

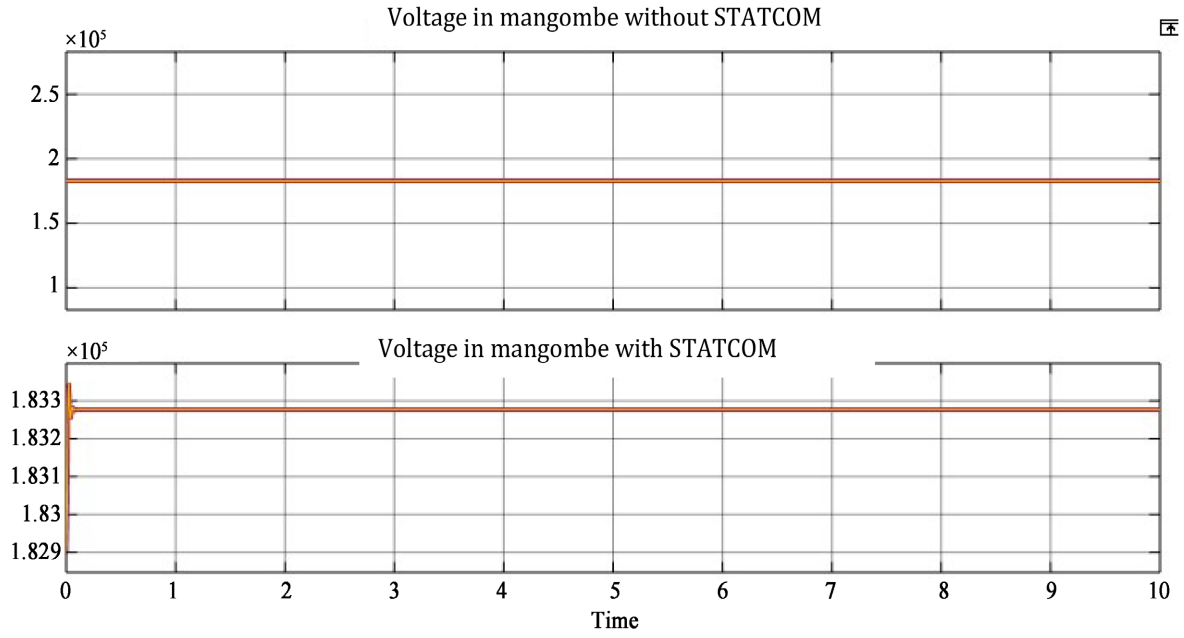

Figure 10. The voltage signal at OYOMABANG before and after insertion of the STATCOM.

marked improvement in the voltage profile, which goes from 157.1 kV to 178.9 kV. However, before the insertion of the STATCOM, the voltage drop was 25.8 kV. This means that the 25.8 kV drop has been reduced to 4.4 kV by the STATCOM and at the same time the power flow has increased and the loads sufficiently supplied (Figure 11 & Table 4).

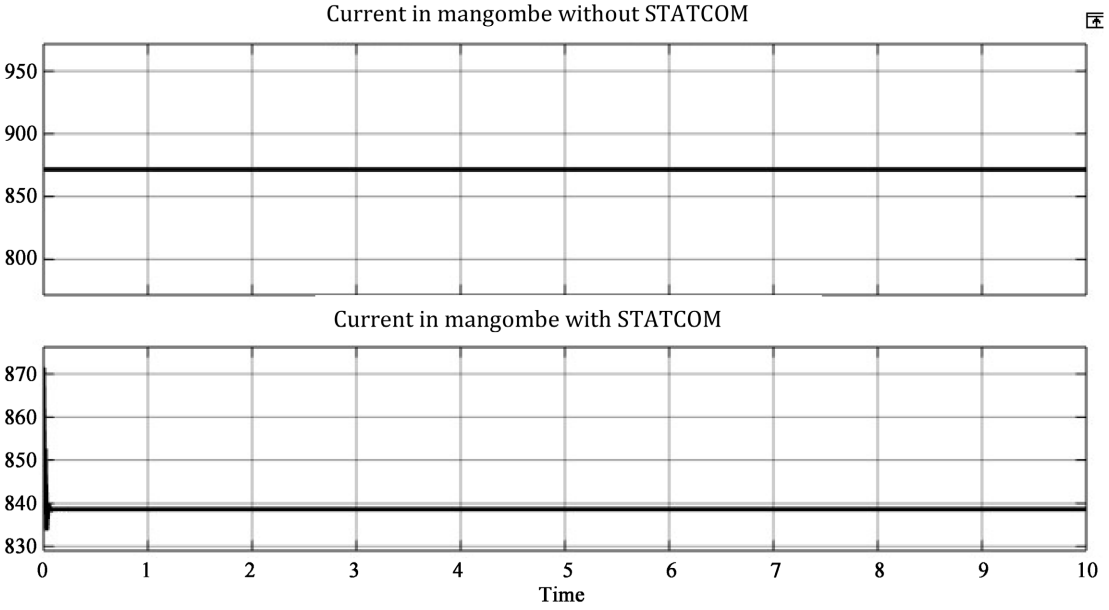

Figure 11. Current at MANGOMBE and at OYOMABANG.

Table 4. Indication of the wattmeters after insertion of the STATCOM.

BUS	Voltage	Active power P	Réactive power Q
MANGOMBE	183.3 kV	2.18×10^8	7.492×10^7
OYOMABANG	178.9 kV	1.138×10^8	6.64×10^7

3.5. Model of the Line with the Statcom in Asymmetrical Operation (Figure 12)

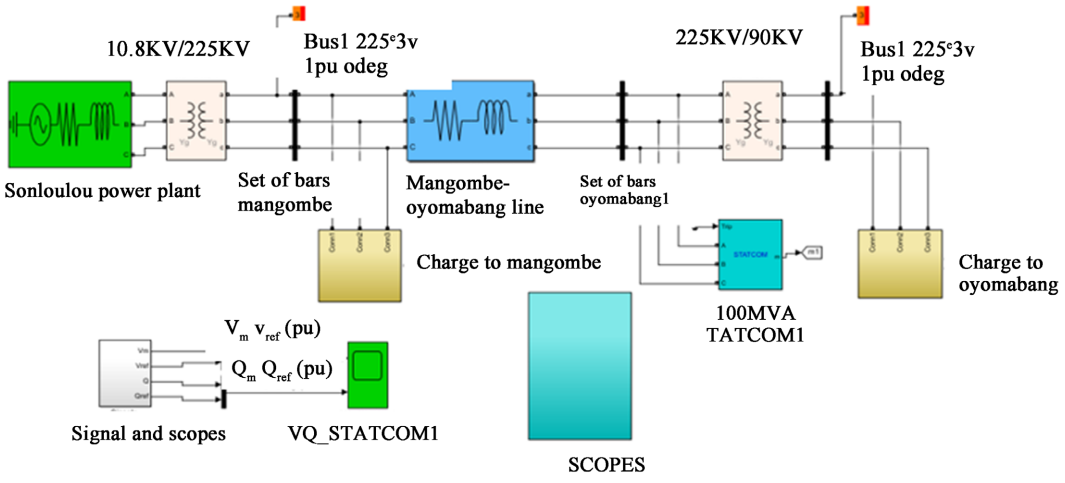

Figure 12. Simulation of the line with STATCOM in asymmetrical operation.

3.6. Voltage Trends before and after Insertion of the STATCOM in MANGOMBE

Figure 13 displays the voltage signal at MANGOMBE before and after insertion of the STATCOM, in asymmetrical operation (single-phase short-circuit), there is an imbalance in the voltage at MANGOMBE. The first graph shows the voltage at MANGOMBE, of the faulty phase Va = 183.3 kV, and of the two other healthy phases Vb = Vc = 182.9 kV, before insertion of the STATCOM. The second graph displays the voltage Va = 183.2 Kv of the faulty phase, and of the two other healthy phases Vb = Vc = 183.3 kV, after insertion of the STATCOM. It can be seen that the STATCOM plays its role of voltage regulation despite the voltage imbalance at MANGOMBE (Table 5).

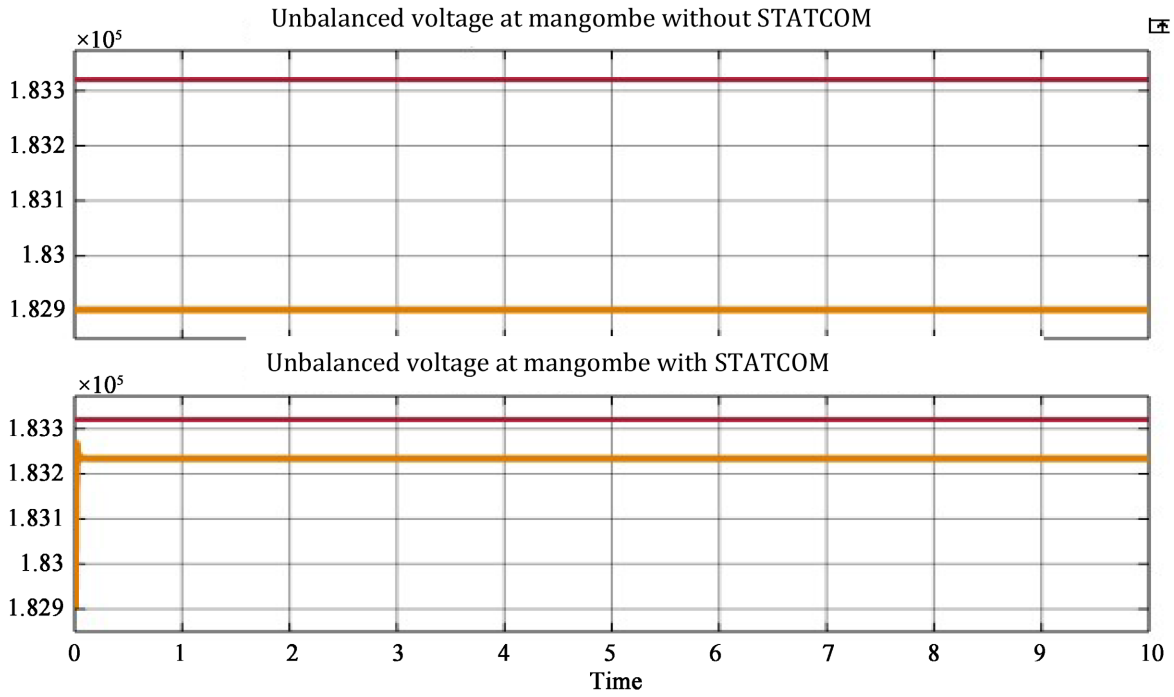

Figure 13. Voltage before and after insertion of the STATCOM in MANGOMBE.

Table 5. Summary of results.

Premises	Voltages without Statcom insertion (kV)	Voltages with insertion Statcom (kV)	Voltages with insertion Statcom, in asymmetric operation (kv)	Active power without Statcom (MW)	Active power with Statcom (MW)	Active power with Statcom, in operation Asymétrique (MW)	Reactive power without Statcom (MW) (MVar)	Active power with Statcom (MW) (MVar)	Reactive power without Statcom (MVar) in asymmetric operation
MANGOMBE	182.9	183.3	Va = 183.3 Vb = 183.2 Vc = 183.2	191	218	100.4	143.9	749.2	8.119
OYOMABANG	157.1	178.9	Va = 132.2 Vb = 177.3 Vc = 177.3	87.72	113.8	95.24	51.18	66.4	55.55

Before insertion of the STATCOM, the rms voltages measured between phase-phase at the busbars were lower than the default admissible value (±10). After inserting the STATCOM, we see a marked improvement in the voltage profile.

The table above presents a summary of the results obtained before and after the insertion of the STATCOM. It can be seen that the STATCOM provides good voltage regulation by generating or absorbing reactive power on the bus to which it is connected, thus improving the voltage profile at OYOMABANG.

The statcom generates a voltage in phase with the network, which is why the voltage of phase A, Va is increased from 0 kV to 132.2 kV. Also generating reactive power to improve the voltage profile at OYOMABANG. This counterpart of the line remains unbalanced and the imbalance is passed on to the loads.

3.7. Model of the Line Equipped with Two Dual IPCs

Figure 14 below presents the simulation of our transmission line equipped with two RPI 240 with three branches, for the Asymmetrical compensation of the line. Each branch is equipped with three reactances for the compensation of the direct and reverse sequence, the compensation of the homopolar sequence cannot be done in the same block, if it consists in directing the homopolar currents towards the earth, it will be done with the Yd transformers at source and load (TH1 and TH2) as we saw in chapter two. The simulation of this line

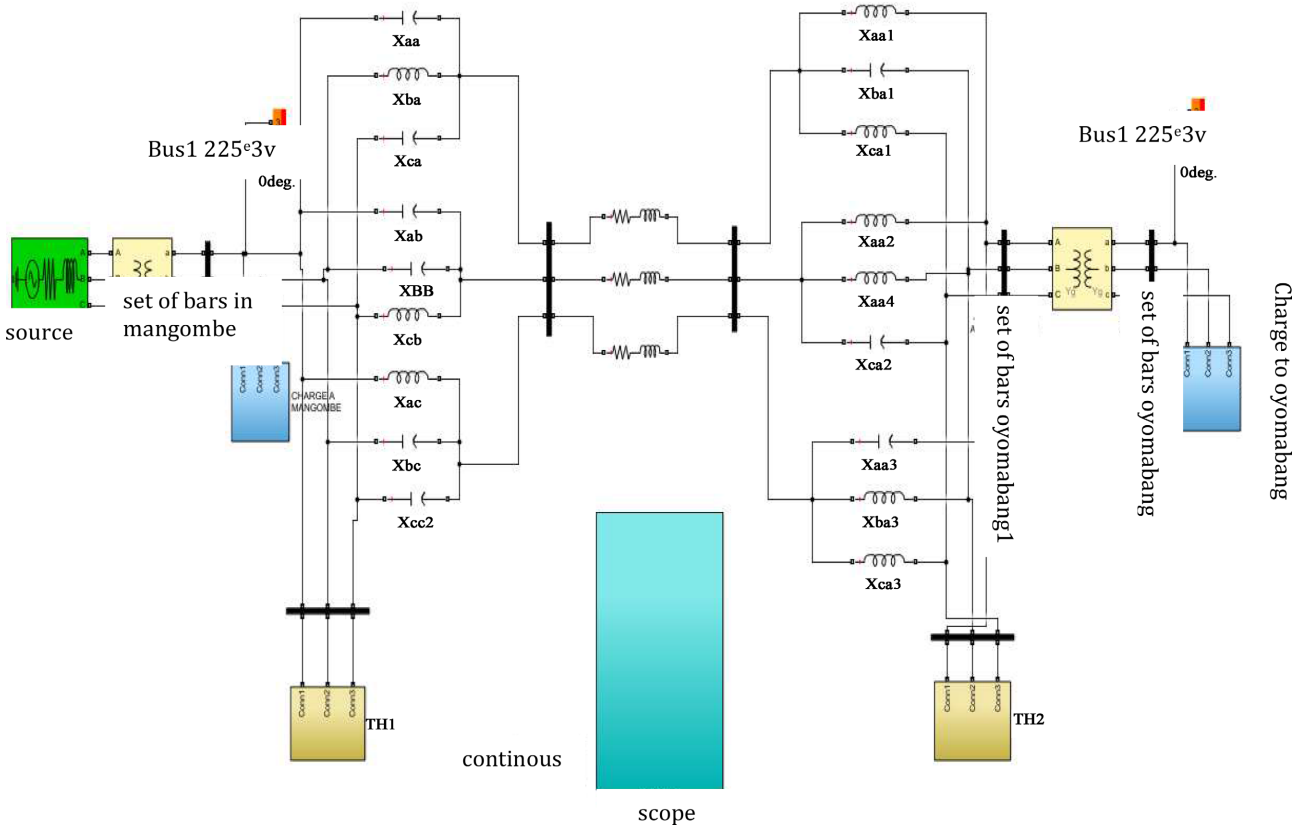

Figure 14. Model of the line in the absence of contingency.

gave the following results.

Voltage curves at the input and at the output of each IPC.

3.8. Shapes of the Voltage at the Input and at the Output of Each IPC (Figure 15)

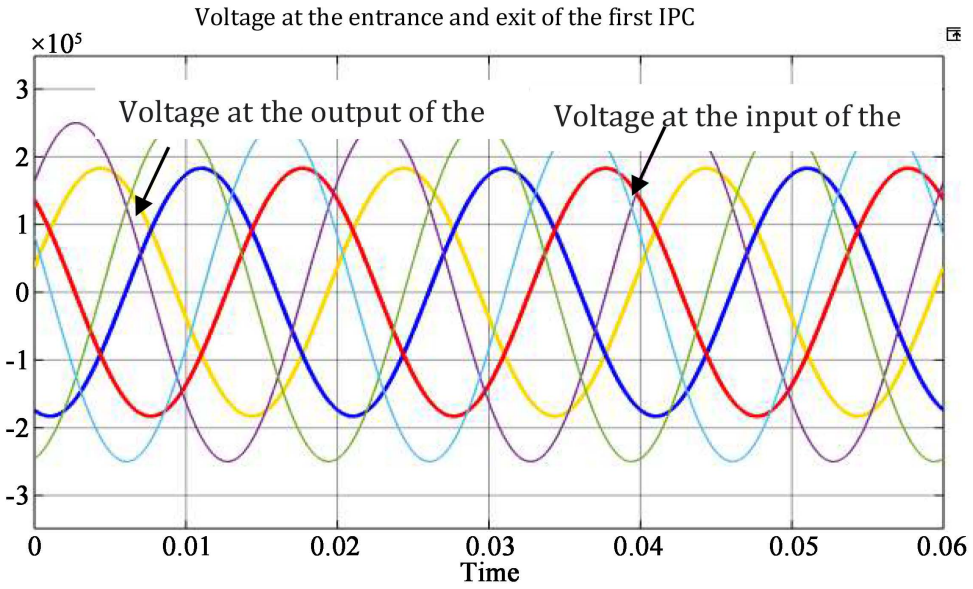

Figure 15. Voltage at the input and output of the 1st IPC.

3.9. Current Samples (Figure 16)

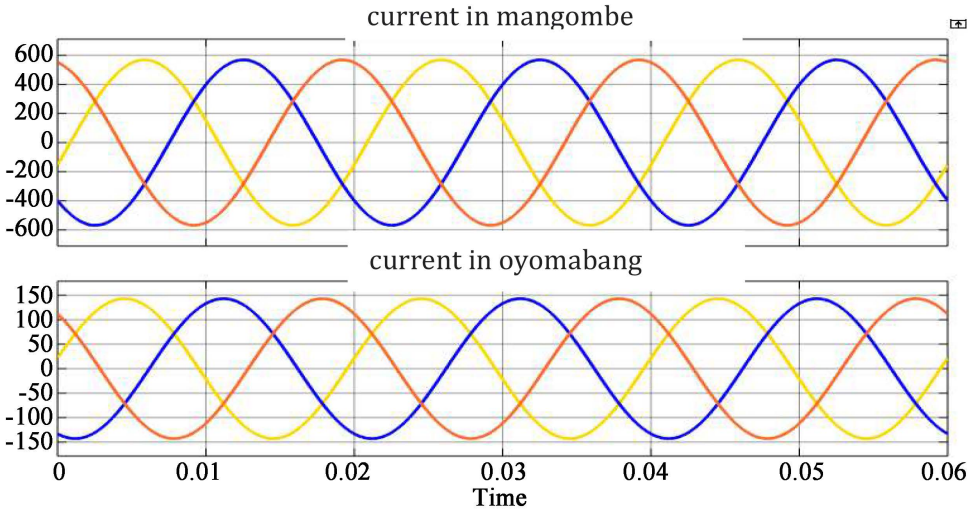

Figure 16. Pre-contingency source and load intensity.

In the absence of an incident, the phase voltage angle in the sub-network:

- 1st RPI entry: 11.66˚ → 1st RPI exit: 97.84˚.
- 2nd RPI input: 90.48˚→load: 0.32˚.

The angle difference between the output of the 1st RPI and the input of the 2nd RPI is due to the inductance of the line while that between the input of the 1st

RPI and the load represents the load angle thus restored.

In the figure, it is clear that the second RPI allows to restore the angle of the source current intensity.

3.10. Simulations of the Contingency Line (Phase A)

Figure 17 presents the simulation of the line in contingency as well as the reconfiguration of the IPCs after a single-phase short circuit.

3.10.1. Voltage Samples

During the contingency, the voltages on the side of the energy source and the load are sinusoidal

Figure 18(a) displays the three-phase signal of the voltage at the level of the MANGOMBE busbar (source side). Figure 18(b) displays the contingency line voltage signal (single-phase short-circuit) before IPC compensation. Cancellation of phase A voltage (faulty phase) is observed. Figure 18(c) displays the voltage signal at the output of the 1st IPC, and Figure 18(d) displays the voltage signal at the output at the input of the 2nd IPC.

Figure 18(e) displays the load voltage signal at OYOMABANG in contingency (single-phase short circuit) after IPC compensation. It can be seen that after compensation of the RPIs, the pre-contingency values are found at the load.

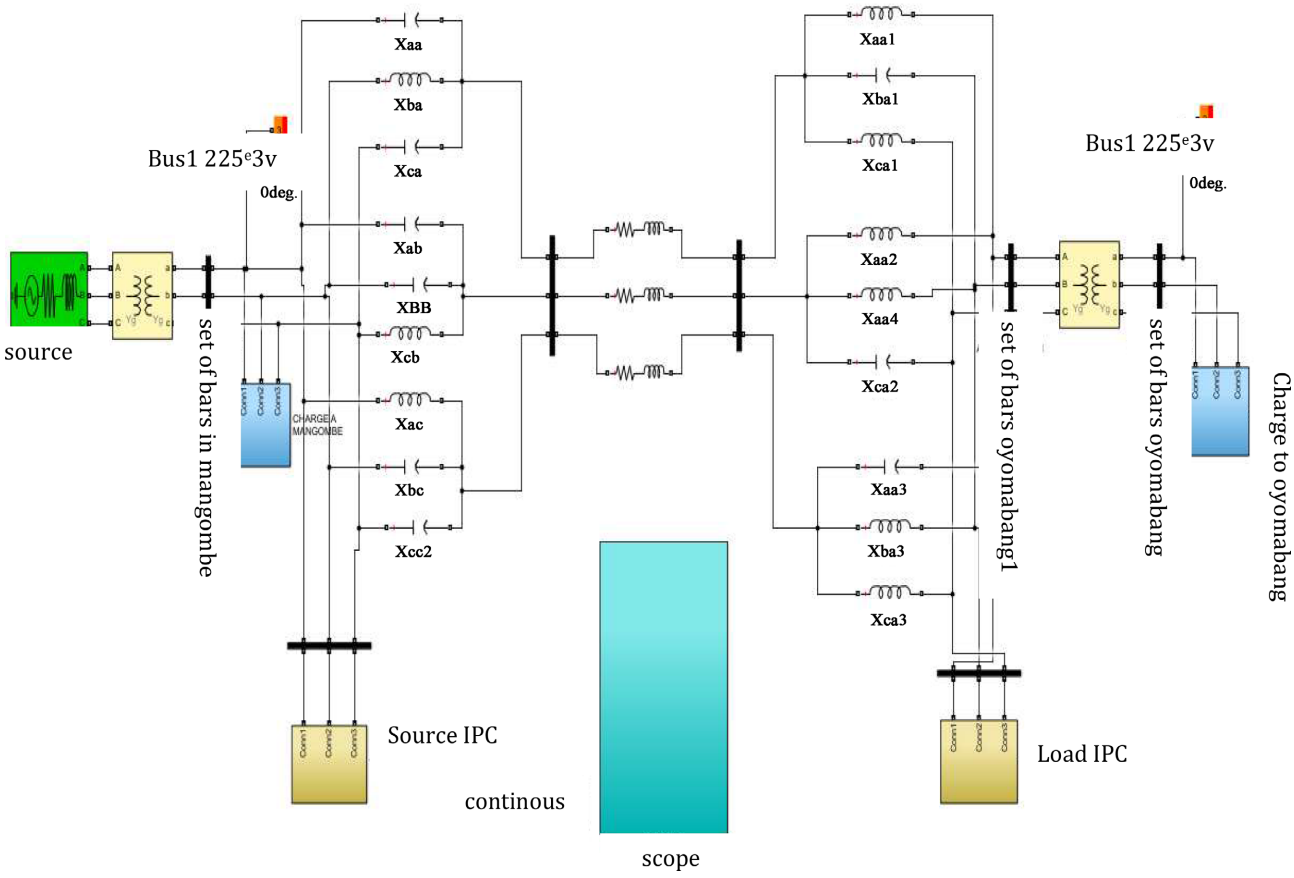

Figure 17. Contingency transmission line/asymmetric IPC compensation.

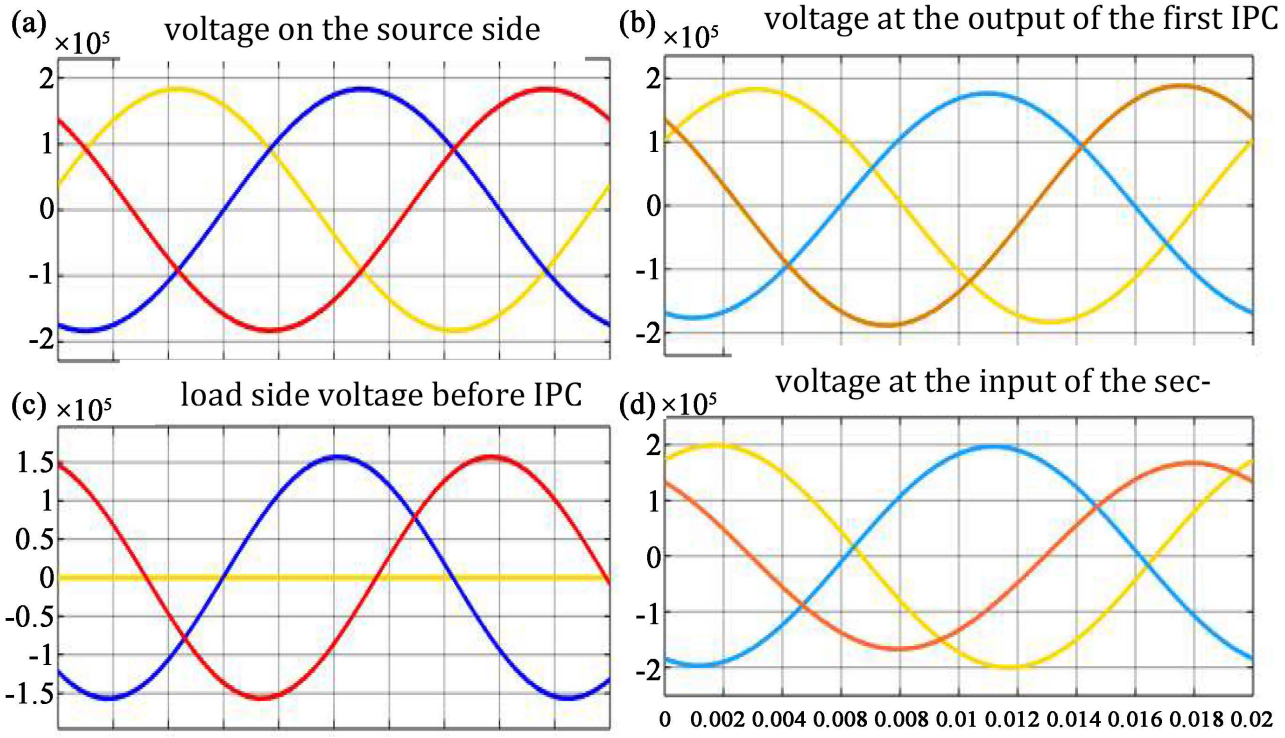

Figure 18. Samples of the voltage evolution at the source/load as well as the voltage at the output of the 1st RPI and the input of the 2nd IPC.

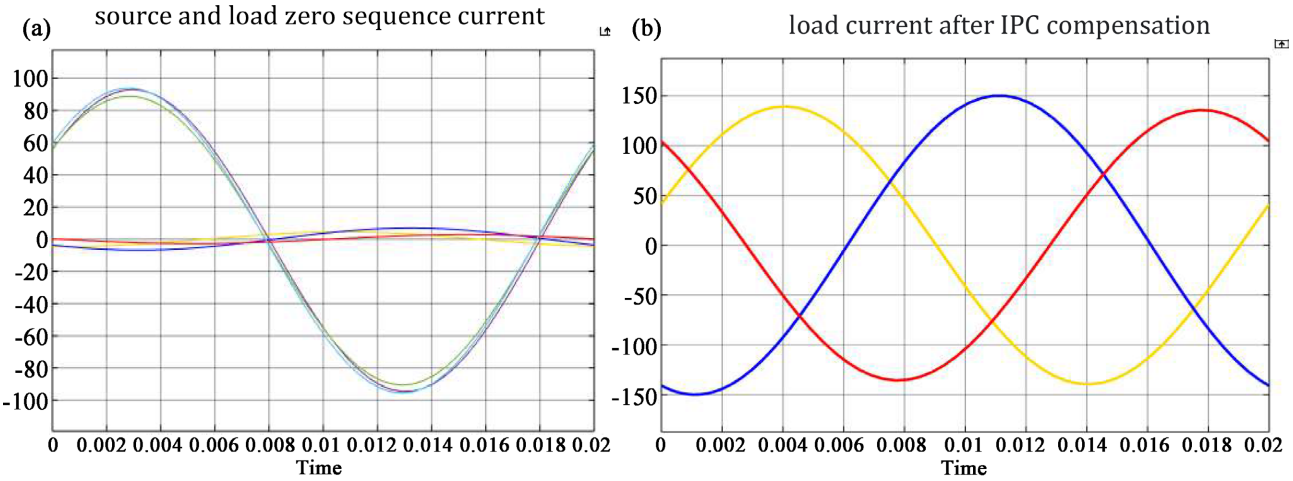

Figure 19. Samples of the evolution of intensities at the source/load.

3.10.2. Intensity Samples

Figure 19(a) shows the intensity of current in line during the contingency, from where after opening of the phase A by the circuit breakers D1 and D4, the intensity of current becomes null. Then the two other phases are the seat of the energy transited between the two nodes of the network. The transmission line thus enters an unbalanced asymmetrical operation.

The source RPI will therefore perform forward, reverse, and zero-sequence compensation at the source. As well as the load RPI which will do the same thing

on the load side. This thus makes it possible to cancel the inverse and homopolar component, and to raise the positive sequence component of the system, and to find the pre-contingency values.

Figure shows the current to the load after compensation of the inverse sequence, Figure 1 shows the homopolar current which goes to ground.

Figure shows the current at the load after complete compensation by the two IPCs.

After this compensation, it appears that the voltage of the load returns to its pre-contingency value. The source and load currents have a slight difference between the amplitudes.

3.11. Simulation of the Contingency Line (Phase A and B)

Figure 20 presents the simulation of the line in contingency as well as the reconfiguration of the IPCs after a two-phase short-circuit. We also note the opening of the reactances which is not necessary for compensation. The compensation of the inverse sequence is carried out by the three reactances of phase A, the compensation of the direct sequence is carried out by the reactances X_CCs and X_CCr of the healthy phases. The results obtained in contingency are presented in Figure 21 and Figure 22 for a contingency on phase A and B.

Voltage samples.

Figure 21 displays the three-phase voltage signal at the MANGOMBE busbar (source side), as well as the voltage at OYOMABANG after compensation for the IPCs. There is a slight difference in the amplitudes of the contingency phases (A and B) with respect to the amplitudes of the source voltage.

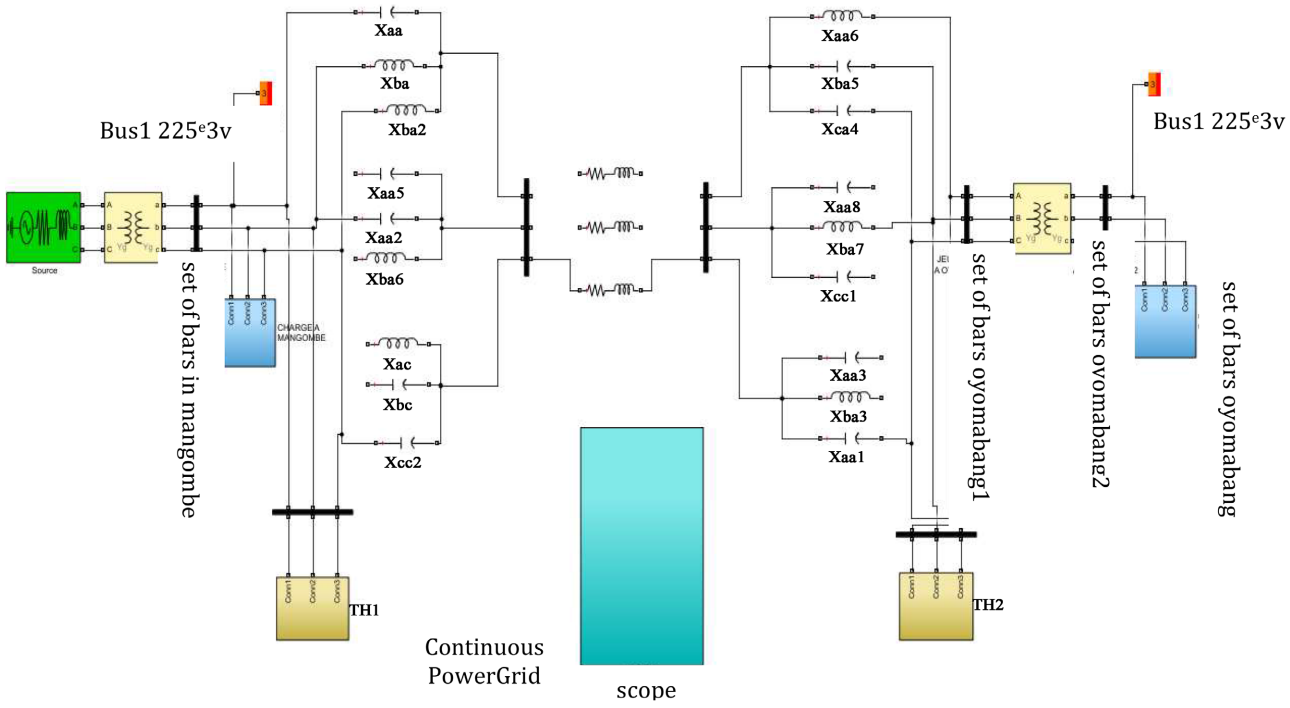

Figure 20. Transmission line in contingency (loss of conductors A and B).

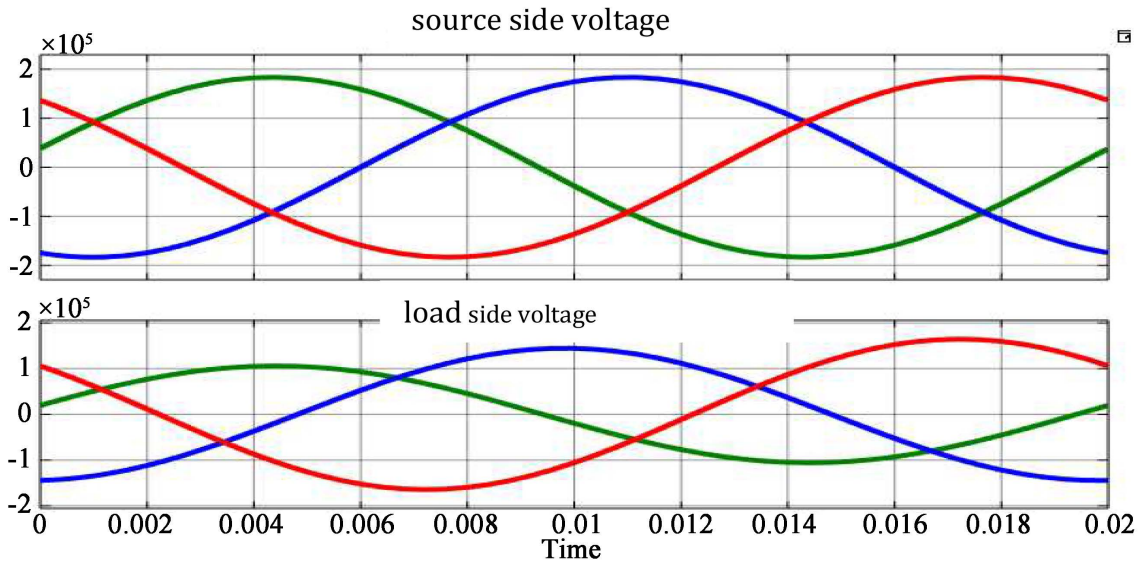

Figure 21. Samples of the voltage evolution at the source/load.

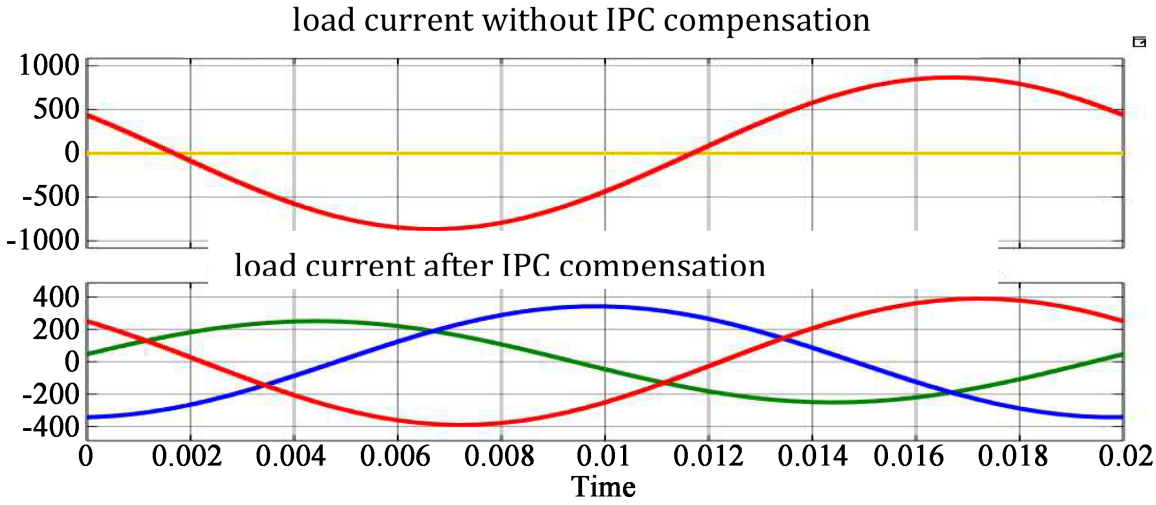

Figure 22. Samples of intensities before and after compensation.

Figure 22 shows the line current intensity during the contingency, hence after opening of phases A and B by the circuit breakers, the current intensity becomes zero on these phases. Then the healthy phase is the seat of the energy transited between the two nodes of the network. The transmission line thus enters an unbalanced asymmetrical operation.

The source RPI will therefore perform forward, reverse, and zero-sequence compensation at the source. As well as the load RPI which will do the same thing on the load side. This thus makes it possible to cancel the inverse and homopolar component, and to raise the positive sequence component of the system, and to find the pre-contingency values.

After this compensation, it appears that the voltage and the current have a slight difference between the amplitudes, compared to the pre-contingency value. The imbalance is not completely canceled.

4. Conclusions

The presented work shows the contribution of STATCOM and the interphase power controller in solving the problems encountered by the network manager. To achieve this, we first highlighted the particularities of the STATCOM and the IPC; then we carried out several simulation tests on the Mangombe-Oyomabang line in the presence of the STATCOM in symmetrical and asymmetrical operation, and then for the three-branch 240 duals IPC.

The simulation of the line in presence of STATCOM in asymmetrical operation allows us to note that in spite of the too important unbalance of the voltage at OYOMABANG. The STATCOM ensures a regulation by phase of the voltage regulation role, thus allowing to reduce the unbalance. The simulations of the line absence of defect in the presence of IPC 240 duals with three branches, made it possible to show that during this period the reactances of each IPC for the weak angles of load, adapt themselves to the variation of this angle.

Conflicts of Interest

The authors declare no conflicts of interest regarding the publication of this paper.

References

[1] Lilien, J.-L. (2009) Transport et distribution de l'énergie électrique. Course Given at the Institute of Electricity Montefiore University of Liege.

[2] Ndjeng Ossono, E. (2014) Electricity in Cameroon: What Is the Way Forward? Denis & Lenora Foretia Foundation, 11.

[3] Sana, A.-R., McGillis, D., Marccau, R., Do, X. and Olivier, G. (2000) Asymmetrical Operation of Corridor with One Single Line. In 2000 *Canadian Conference on Electrical and Computer Engineering. Navigating to a New Era* (*Cat. No.* 00*TH*8492), **2**, 936-940.

[4] Steinmetz, C.P. (1916) Theory and Calculation of Alternating Current Phenomena. McGraw-Hill Book Company, Incorporated, New York.

[5] Asma, B. and Soumia, D. (2019) Control of an SSSC by Neural Networks to Improve the Static Behavior of an Electroenergetic System. Master Thesis, University Ziane Achour of Djelfa, Djelfa.

[6] Brochu, J., Pelletier, P., Beauregard, F. and Morin, G. (1994) The Interphase Power Controller: A New Concept for Managing Power Flow within AC Networks, IEEE *Transactions on Power Delivery*, **9**, 833-841. https://doi.org/10.1109/61.296264

[7] Léandre, N.N., Koko, J., Ndjakomo Essiane, S. and Batassou Guilzia, J. (2021) Comparative Analysis of Hybrid Controllers of FACTS Systems (UPFC) and Interphase Power Controllers Type RPI 30P15 on the Management of Electrical Network Contingencies. *World Journal of Engineering and Technology*, **9**, 708-726.

[8] Oldeen, J. and Sharma, V. (2020) Reinforcement Learning for Grid Voltage Stability with FACTS. Degree of Master, Uppsala University.

[9] Kom, C.H., Mandeng, J.-J. (2020) Understanding Interphase Power Controller: A Description. *Journal of Electrical Engineering, Electronics, Control and Computer Science*, **6**, 19-24.

[10] Grunbaum, R., Noroozian, M., and Thorvaldsson, B.J.A.R. (1999) FACTS—Powerful Systems for Flexible Power Transmission. *ABB Review*, No. 5, 4-17.

[11] Shahraki, E.G. (2003) Apport de l'UPFC à l'amélioration de la stabilité transitoire des réseaux électriques. PhD Thesis, Université Henri Poincaré-Nancy 1.